



ELSEVIER

23 September 1994

**CHEMICAL  
PHYSICS  
LETTERS**

Chemical Physics Letters 227 (1994) 617–622

## Transient Raman spectroscopy of $^{15}\text{N}$ -substituted bacteriochlorophyll a. An empirical assignment of $T_1$ Raman lines

Leenawaty Limantara <sup>a</sup>, Yasushi Koyama <sup>a</sup>, Ingrid Katheder <sup>b</sup>, Hugo Scheer <sup>b</sup><sup>a</sup> Faculty of Science, Kwansai Gakuin University, Uegahara, Nishinomiya 662, Japan<sup>b</sup> Botanisches Institut der Universität München, D-80638 Munich, Germany

Received 16 May 1994; in final form 23 June 1994

### Abstract

$^{15}\text{N}$ -substituted bacteriochlorophyll a (BChl a) was extracted from the cells of *Rhodobacter sphaeroides* 2.4.1 grown in a medium containing  $^{15}\text{N}$ -ammonium sulfate and yeast concentrate. The  $T_1$  Raman spectra of  $^{14}\text{N}$ - and  $^{15}\text{N}$ -BChl a were obtained as the difference spectra of high-power minus low-power of one-color, pump-and-probe measurements using 420 nm, 5 ns pulses. A set of empirical assignments of the  $T_1$  Raman lines was made, based on shifts upon  $^{14}\text{N} \rightarrow ^{15}\text{N}$  substitution. The  $S_0$  Raman spectra of the two BChls were also obtained by using the 457.9 nm cw beam, and a set of assignments of the  $S_0$  Raman lines was given for comparison.

### 1. Introduction

Bacteriochlorophylls (BChl) in excited states play important roles in bacterial photosynthesis: The  $S_1$  state is responsible for singlet energy transfer in light-harvesting complexes (LHC) and for charge separation at the special pair in the reaction center (RC). On the other hand, the  $T_1$  state is generated at the special pair by charge recombination under reducing conditions, and the triplet energy is transferred, via one of the accessory BChls, to the carotenoid (Car) to be dissipated [1,2]. In the triplet energy transfer reaction to the Car, the electronic and molecular structure of  $T_1$  state BChl must be most important, since the overlap of the LUMOs and the HOMOs is a crucial factor for the reaction to take place.

Changes in the bond order in the macrocycle of BChl a, upon excitation, have been shown by transient Raman spectroscopy, a decrease (increase) in

the bond order for a bond with a double-bond (single-bond) character has been predicted based on changes in Raman frequencies upon excitation to both the  $T_1$  [3] and  $S_1$  [4] states. Here, comparison of the Raman frequencies was based on the assumption that no drastic changes should take place in the bond order. Thus, a pair of Raman lines with the nearest frequencies were correlated between the ground state and the excited state in question.

Since BChl molecules with exactly the same structural formula play different roles depending on the binding site in pigment-protein complexes, the excited-state structures and properties must be controlled by intermolecular interaction with apo-protein(s) and/or nearby pigment(s). From this viewpoint, solvent effects on  $T_1$  state BChl a have been examined by transient Raman spectroscopy [5,6], and the penta- and hexa-coordinated monomeric states as well as the penta-coordinated aggre-

gated state were differentiated by the use of 'the ring-breathing mode' in the  $T_1$  state.

The above two sets of conclusions critically depend on the assignment of the excited-state Raman lines. The assumption of no drastic changes in the bond order upon triplet excitation was not warranted in linear polyenes (retinoids and carotenoids). Upon excitation to the triplet state, large changes in the bond order, toward inversion, take place in the central part of a conjugated chain, which we call 'the triplet-excited region', although the bond order in the  $S_0$  state is conserved at both ends [7,8]. Such drastic changes in the electronic and molecular structure may take place in BChl **a** as well.

In order to examine this issue by characterizing each Raman line, the most powerful technique is isotope substitution which was successfully applied to  $S_0$  state BChl **a** by Lutz [9]. In the present investigation, we have attempted to record the  $T_1$  and  $S_0$  Raman spectra of  $^{14}\text{N}$ - and  $^{15}\text{N}$ -BChl **a** in order to answer the following two questions. (1) How can the  $T_1$  and  $S_0$  Raman lines be assigned empirically based on isotope substitution? (2) How does the  $T_1$  Raman spectrum compare with, or contrast to, the  $S_0$  Raman spectrum?

## 2. Experimental

Cells of *Rhodobacter sphaeroides* 2.4.1 were grown in the rhodospirillaceae medium [10], in which 0.1 g/l  $^{14}\text{NH}_4\text{Cl}$  was replaced by 0.2 g/l  $(^{15}\text{NH}_4)_2\text{SO}_4$  (Sigma-Aldrich, 98 at%) and yeast extract was replaced by yeast concentrate (Sigma) [11].  $^{15}\text{N}$ -substituted bacteriochlorophyll **a** ( $^{15}\text{N}$ -BChl **a**) was extracted from the cells with methanol in the dark under nitrogen atmosphere. It was transferred to the mixed ether layer by partitioning between petroleum ether/diethyl ether (1:2 v/v) and water. After drying, it was purified by column chromatography using Sepharose CL-6B as the stationary phase, and 2-propanol/*n*-hexane (1:20 v/v) as the eluent. Analysis by HPLC of  $^{15}\text{N}$ -BChl **a** thus obtained showed a single peak (detection at both 355 and 435 nm).  $^{14}\text{N}$ -BChl **a** was obtained as described previously [3].

The  $T_1$  Raman spectrum was obtained in acetone solution ( $3 \times 10^{-3}$  M, sealed under nitrogen atmo-

sphere in an ampule and rotated) by a one-color experiment using the 420 nm pulses (duration 5 ns and repetition 10 Hz) as the difference spectrum which was obtained by subtracting a low-power spectrum (0.3 mJ/pulse) from a high-power spectrum (2.0–2.4 mJ/pulse). The authentic  $S_0$  Raman spectrum was obtained in acetone solution ( $9 \times 10^{-3}$  M) by the use of the cw 457.9 nm beam of an  $\text{Ar}^+$ -ion laser (17 mW). The details were described previously [3,6]. Spectral smoothing was performed for both the  $T_1$  and  $S_0$  Raman spectra.

The substitution of  $^{15}\text{N}$  at each nitrogen site, i.e.  $x = [^{15}\text{N}] / ([^{15}\text{N}] + [^{14}\text{N}])$ , was determined as follows. (1) Four  $^{15}\text{N}$  peaks in the NMR spectrum of  $^{15}\text{N}$ -BChl **a** showed equal intensity, a fact which indicates equal substitution at the four nitrogen sites in BChl **a**. (2) A mass spectrum of  $^{14}\text{N}$ -BChl **a** showed a series of peaks with the interval of one mass unit originating from the molecular ion of BChl **a**,  $M^+$ , and those of  $(M-1)^+$ ,  $(M-2)^+$ , ... and  $(M+1)^+$ ,  $(M+2)^+$ , ... due to the abstraction and addition of hydrogen by the solvent, *m*-nitro-benzyl-alcohol. (3) A mass spectrum of  $^{15}\text{N}$ -BChl **a** showed a series of peaks, the changes in the relative intensity of which were ascribed to the generation of a series of isotope species in the ratio,  $^{15}\text{N}_4: ^{15}\text{N}_3^{14}\text{N}_1: ^{15}\text{N}_2^{14}\text{N}_2: ^{15}\text{N}_1^{14}\text{N}_3: ^{14}\text{N}_4 = 0.09: 0.24: 0.32: 0.22: 0.13$ , which lead to a value of  $x$  of approximately 0.55. The distribution of various molecular ions was assumed to be the same between  $^{14}\text{N}$ -BChl **a** and  $^{15}\text{N}$ -BChl **a**.

## 3. Results and discussion

### 3.1. Efficient preparation of $^{15}\text{N}$ -BChl **a**

Growth conductions (complete consumption of oxygen in the medium before starting irradiation, moderate light intensity and a temperature of 30°C) to keep the cells of *Rhodobacter sphaeroides* active turned out to be most important in  $^{15}\text{N}$  incorporation; much better results were obtained for the wild type 2.4.1 than for a carotenoidless mutant R26.1. The cells were adapted for a couple of transfers (5–7 days of incubation each time) to the medium containing ammonium sulfate and yeast concentrate. In order to enhance the  $^{15}\text{N}$  enrichment, the amount of

the nitrogen source was reduced to 40% before culturing the cells in the medium containing  $(^{15}\text{NH}_4)_2\text{SO}_4$ .

In order to increase the yield in the purification procedure of  $^{15}\text{N}$ -BChl a, the conditions in the column chromatography were carefully controlled so that pure  $^{15}\text{N}$ -BChl a could be obtained without further purification by HPLC. A typical extraction and purification procedure to obtain 150–200 mg of  $^{15}\text{N}$ -BChl a from 40 g cells took less than 5 h; this rapid procedure strongly prevented degradation of BChl a.

### 3.2. Isotope shifts and assignment of Raman lines in the $S_0$ state

Fig. 1 shows the chemical structure of BChl a together with the atom typification used. The macrocycle has the bacteriochlorine skeleton containing two unsaturated rings (rings I and III) and two saturated rings (rings II and IV); an additional saturated ring (ring V) is attached to ring III. All the C–C and C–N stretchings in the macrocycle are expected to be coupled with one another to form a set of normal modes.

Nishizawa and Koyama [3] attempted to estimate the  $\pi$ -bond order of each bond in the bacteriochlorine skeleton based on a set of resonance structures,

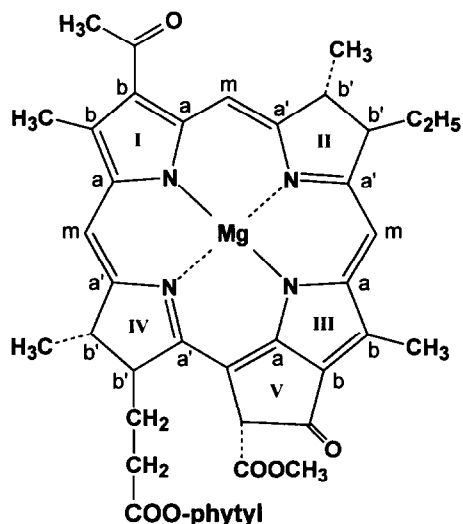


Fig. 1. The chemical structure of bacteriochlorophyll a (BChl a) and typification of atoms.

and predicted the intrinsic frequencies of the stretching vibrations in the following order:  $C_{a'}-C_m > C_b-C_b = C_a-C_b > C_a-C_m = C_{a'}-N > C_a-N$ . Donohoe et al. [12] calculated the normal vibrations of the BChl a model by the QCFF/PI method. Here, the differentiation between the  $C_{a'}-C_m$  and  $C_a-C_m$  ( $C_{a'}-N$  and  $C_a-N$ ) stretchings turned out to be of no practical significance because of strong coupling between them. The coupled stretching vibrations appeared in the following order: the  $C_a-C_m$  stretchings ( $1650-1540\text{ cm}^{-1}$ ) > the  $C_b-C_b$  stretchings ( $1620-1520\text{ cm}^{-1}$ ) > the  $C_a-C_b$  stretchings ( $1530-1430\text{ cm}^{-1}$ ) > the  $C_a-N$  stretchings ( $1390-1280\text{ cm}^{-1}$ ) > the  $C_m-H$  deformations ( $1280-1200\text{ cm}^{-1}$ ) > the  $C_a-N$  stretchings ( $1200-1100\text{ cm}^{-1}$ ). (The  $C_a-N$  stretchings were split into two separate regions.)

The Raman spectra of monomeric and oligomeric BChl a at 30 K probed at 363.8 nm have been reported by Lutz and Robert [13] and Lutz [9], and a set of empirical assignment of the Raman lines for the entire spectral region was proposed on the basis of the  $^{14}\text{N} \rightarrow ^{15}\text{N}$  and  $^{24}\text{Mg} \rightarrow ^{26}\text{Mg}$  substitutions [9].

The above theoretical and experimental results obtained so far, together with the shifts upon the  $^{14}\text{N} \rightarrow ^{15}\text{N}$ , will be used in the following empirical assignments of the  $S_0$  and  $T_1$  Raman lines.

Fig. 2 shows the  $S_0$  Raman spectra of (1)  $^{14}\text{N}$ - and (2)  $^{15}\text{N}$ -BChl a. The pattern of the present spectrum

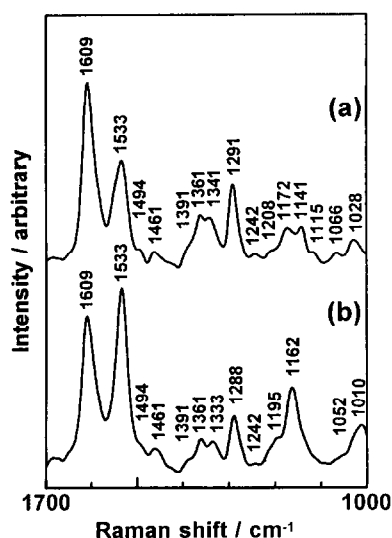


Fig. 2. The  $S_0$  Raman spectra of (a)  $^{14}\text{N}$ - and (b)  $^{15}\text{N}$ -BChl a.

of  $^{14}\text{N}$ -BChl **a** (457.9 nm excitation, in acetone solution, and at room temperature) is slightly different from that reported by Lutz and Robert [13] (363.8 nm excitation, in methylimidazole, and at 30 K), although major Raman lines are observed in common in these spectra. The difference must originate from the different wavelengths of probing (supported by the measurement of an excitation profile), the amount of substitution, and from the spectral resolution which depends also on the temperature. (The Raman spectra of  $^{14}\text{N}$ - and  $^{15}\text{N}$ -BChl **a** probed by the 420 nm pulses with low photon density (low lasing power and defocused beam) should represent the  $S_0$  Raman spectra. The spectral patterns (data not shown) are similar to, but definitely different from, those of Fig. 2. This is due to the different wavelength of probing, and also due to some contribution of the  $T_1$  species generated by the pulsed excitation.)

Fig. 3a compares schematically the authentic  $S_0$  Raman lines (probed by the cw 457.9 nm beam) between the  $^{14}\text{N}$ - and  $^{15}\text{N}$ -BChl **a**. The  $S_0$  Raman lines of  $^{14}\text{N}$ -BChl **a** can be classified into two groups based on the shifts upon  $^{14}\text{N} \rightarrow ^{15}\text{N}$ -substitution and assigned as follows.

(a) Raman lines which are not affected by the isotope substitution. The line at  $1609\text{ cm}^{-1}$  should be definitely assigned to the  $\text{C}_a\text{-C}_m$  stretching, while the  $1533\text{ cm}^{-1}$  line can be assigned to the  $\text{C}_b\text{-C}_b$  (probably coupled with  $\text{C}_a\text{-C}_b$ ) stretching. The  $1494$  and  $1461\text{ cm}^{-1}$  lines can be assigned to the  $\text{C}_a\text{-C}_b$  (coupled with  $\text{C}_b\text{-C}_b$ ) stretchings. Finally, the  $1391$ ,  $1361$  and  $1242\text{ cm}^{-1}$  bands may be assigned to the  $\text{C}_m\text{-H}$  deformations.

(b) Raman lines which are shifted by the isotope substitution. A shoulder at  $1549\text{ cm}^{-1}$  and the lines at  $1341$  and  $1291\text{ cm}^{-1}$ , all of which are shifted to the lower frequencies by the isotope substitution, are to be related to the  $\text{C}_a\text{-N}$  stretchings. Medium and weak Raman lines in the  $1230\text{--}1000\text{ cm}^{-1}$  are strongly affected by the isotope substitution, which is probably due to the presence of variously  $^{15}\text{N}$ -substituted species. It is almost impossible to correlate any pair of the Raman lines between  $^{14}\text{N}$ - and  $^{15}\text{N}$ -BChl **a**, and to define 'the isotope shifts' as has been done by Lutz [9].

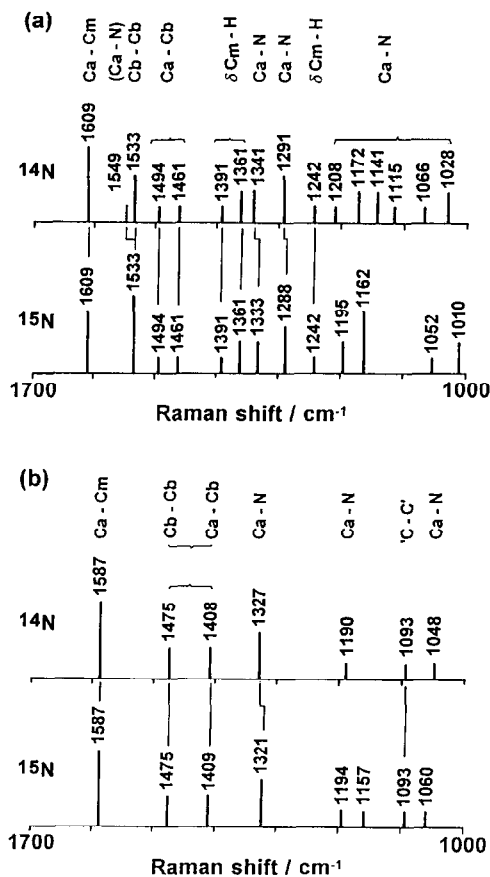


Fig. 3. A schematic presentation of (a) the  $S_0$  and (b) the  $T_1$  Raman lines of  $^{14}\text{N}$ - and  $^{15}\text{N}$ -BChl **a**. A pair of empirical sets of assignments are also given.

### 3.3. Isotope shifts and assignment of Raman lines in the $T_1$ state

Fig. 4 shows the  $T_1$  Raman spectra of  $^{14}\text{N}$ - and  $^{15}\text{N}$ -BChl **a**. Fig. 3b compares schematically their Raman lines. The  $T_1$  Raman lines of  $^{14}\text{N}$ -BChl **a** also can be classified into two groups based on the isotope shifts and assigned as follows.

(a) Raman lines which are not affected by the isotope substitution. The line at  $1587\text{ cm}^{-1}$  should be definitely assigned to the  $\text{C}_a\text{-C}_m$  stretching which we referred to as the ring-breathing mode [5]. It is not shifted by the  $^{14}\text{N} \rightarrow ^{15}\text{N}$  substitution, and the in-phase stretching of the  $\text{C}_a\text{-C}_m$  (and  $\text{C}_a'\text{-C}_m$ ) bonds is expected to give rise to this high Raman intensity. The  $1475$  and  $1408\text{ cm}^{-1}$  lines can be assigned to the  $\text{C}_b\text{-}$

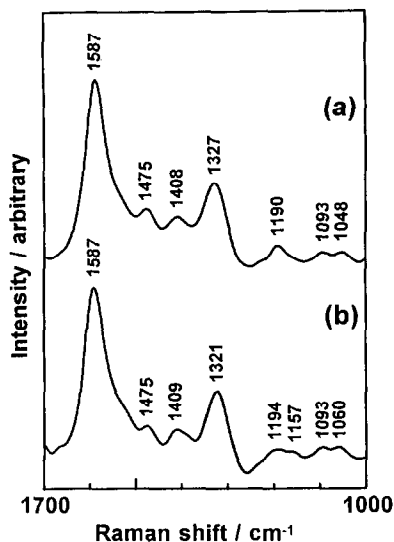


Fig. 4. The  $T_1$  Raman spectra of (a)  $^{14}\text{N}$ - and (b)  $^{15}\text{N}$ -BChl a.

$C_b$  and  $C_a$ - $C_b$  stretchings, which may be coupled with one another. The Raman line at  $1093\text{ cm}^{-1}$  is assigned to some 'C-C' single-bond ( $C_{b'}$ - $C_{b'}$  and/or  $C_{a'}$ - $C_{b'}$ ) stretching.

(b) Raman lines which are shifted by the isotope substitution. The Raman line at  $1327\text{ cm}^{-1}$ , which shifts to lower frequency upon the isotope substitution, can be assigned to one of the  $C_a$ -N stretchings. The  $1190$  and  $1048\text{ cm}^{-1}$  lines are related to the  $C_a$ -N stretchings. Large changes in the spectral pattern in the region below  $1200\text{ cm}^{-1}$  (except for the  $1093\text{ cm}^{-1}$  line) prevents the correlation of the Raman lines between  $^{14}\text{N}$ - and  $^{15}\text{N}$ -BChl a and also the definition of the isotope shifts; this is probably due to the presence of variously  $^{15}\text{N}$ -substituted species as in the case of the  $S_0$  state.

Thus, two sets of empirical assignments have been given for the  $S_0$  and  $T_1$  Raman lines to answer the first question addressed in Section 1. The Raman lines in the highest frequency region have been characterized as the  $C_a$ - $C_m$ ,  $C_b$ - $C_b$ , and  $C_a$ - $C_b$  stretchings. The present results support the previous conclusion: (1) that a decrease in the bond order takes place, upon triplet excitation, for the C-C bonds with a double-bond character [3], and (2) that the ring-breathing mode reflects the states of coordination and aggregation in  $T_1$  state BChl a [5]. However, the Raman lines in the region below  $1200\text{ cm}^{-1}$  could not be characterized. Therefore, the conclusion that an increase in

the bond order takes place for a C-C or C-N bond with a single-bond character awaits a final proof.

As for the spectral comparison between the  $S_0$  and  $T_1$  states to answer the second question in Section 1, it has been found that the spectral patterns of  $T_1$  state BChl a (Fig. 3b) are much simpler than those of  $S_0$  state BChl a (Fig. 3a). The situation is similar to the case of retinal, which was analyzed in great detail by combination of specific deuterium substitutions and the calculation of normal vibrations (unpublished results). Only selected vibrational modes appear in the  $T_1$  Raman spectrum of retinal; those vibrational modes which take place in 'the central, triplet-excited region' gave rise to high Raman intensity, while those vibrational modes taking place at the peripheral parts did not appear in the  $T_1$  spectrum. The present  $T_1$  Raman spectrum (with fewer Raman lines and the large low frequency-shifts of the carbon-carbon double-bond stretchings) suggests the presence of 'a triplet-excited region' in BChl a as well, although the final conclusion should wait for a detailed analysis by the calculation of normal vibrations for the completely isotope substituted species.

#### Acknowledgement

This work was supported by the Deutsche Forschungsgemeinschaft (SFB 143, project A9). We are indebted to W. Schäfer (Max-Planck-Institut für Biochemie, Martinsried, Germany) for providing us with the mass spectra.

#### References

- [1] H. Scheer and S. Schneider, *Photosynthetic light-harvesting systems: organization and function* (De Gruyter, Berlin, 1988).
- [2] J. Deisenhofer and J.R. Norris, *The photosynthetic reaction center*, Vols. 1 and 2 (Academic Press, New York, 1993).
- [3] E. Nishizawa and Y. Koyama, *Chem. Phys. Letters* 172 (1990) 317.
- [4] E. Nishizawa, H. Hashimoto and Y. Koyama, *Chem. Phys. Letters* 181 (1991) 387.
- [5] E. Nishizawa, L. Limantara, N. Nanjou, H. Nagae, T. Kakuno and Y. Koyama, *Photochem. Photobiol.* 59 (1994) 229.
- [6] E. Nishizawa and Y. Koyama, *Chem. Phys. Letters* 176 (1991) 390.

- [7] Y. Mukai, H. Hashimoto and Y. Koyama, *J. Phys. Chem.* 94 (1990) 4042.
- [8] M. Kuki, Y. Koyama and H. Nagae, *J. Phys. Chem.* 95 (1991) 7171.
- [9] M. Lutz, in: *Advances in infrared and Raman spectroscopy*, Vol. 11, eds. R.J.H. Clark and R.E. Hester (Wiley, New York, 1984) p. 211.
- [10] D. Beese, R. Steiner, H. Scheer, A. Angerhofer, B. Robert and M. Lutz, *Photochem. Photobiol.* 46 (1988) 293.
- [11] A. De Groot, A.J. Hoff, R. De Beer and H. Scheer, *Chem. Phys. Letters* 113 (1985) 286.
- [12] R.J. Donohoe, H.A. Frank and D.F. Bocian, *Photochem. Photobiol.* 48 (1988) 531.
- [13] M. Lutz and B. Robert, in: *Biological applications of Raman spectroscopy*, Vol. 3, ed. T.G. Spiro (Wiley, New York, 1988) p. 347.